Article

Stereospecific NMR Assignments of Prochiral Methyls, Rotameric States and Dynamics of Valine Residues in Malate Synthase G

Vitali Tugarinov, and Lewis E. Kay

J. Am. Chem. Soc., **2004**, 126 (31), 9827-9836• DOI: 10.1021/ja048738u • Publication Date (Web): 16 July 2004

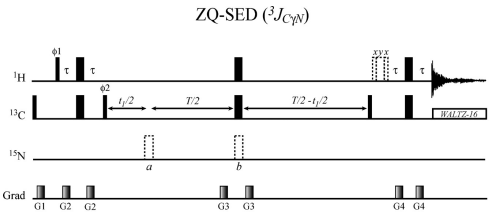

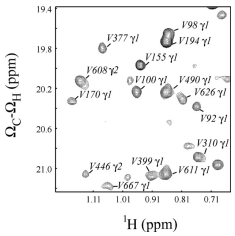

More About This Article

Additional resources and features associated with this article are available within the HTML version:

- Supporting Information
- Links to the 2 articles that cite this article, as of the time of this article download
- Access to high resolution figures
- Links to articles and content related to this article
- Copyright permission to reproduce figures and/or text from this article

View the Full Text HTML

J|A|C|S
ARTICLES
Published on Web 07/16/2004

Stereospecific NMR Assignments of Prochiral Methyls, Rotameric States and Dynamics of Valine Residues in Malate Synthase G

Vitali Tugarinov and Lewis E. Kay*

Contribution from the Protein Engineering Network Centres of Excellence and the Departments of Medical Genetics, Biochemistry, and Chemistry, University of Toronto, Toronto, Ontario, Canada M5S 1A8

Received March 4, 2004; E-mail: kay@pound.med.utoronto.ca

Abstract: Near complete stereospecific assignments of the prochiral methyl carbons of Leu and Val residues in malate synthase G, a 723 residue enzyme, are reported. Assignments were obtained on the basis of a 10% fractional ^{13}C-labeling strategy developed by Wüthrich and co-workers [Neri, D; Szyperski, T; Otting, G; Senn, H; Wüthrich, K. *Biochemistry* **1989**, *28*, 7510−7516] and, in the case of Val residues, supplemented with results from a series of new methyl-TROSY quantitative *J* experiments for measuring $^3J_{C\gamma N}$ and $^3J_{C\gamma C'}$ couplings. The measured ^3J couplings were also used to probe Val side chain dynamics. A strong correlation is observed between rotamer averaging established on the basis of the couplings and side chain millisecond time scale dynamics measured using methyl-TROSY based $^1H-^{13}C$ multiple quantum relaxation dispersion experiments.

Introduction

The development of TROSY-based methods for the assignment of high molecular weight proteins has had a significant effect in lowering the molecular weight barriers that have hampered NMR studies of large systems in the past.[1−4] Using a series of 4D-TROSY triple resonance experiments,[5,6] our laboratory has succeeded in assigning over 95% of the backbone ^1HN, ^{15}N, $^{13}C^{\alpha}$, $^{13}C'$ and the side chain $^{13}C^{\beta}$ chemical shifts of malate synthase G (MSG), an 82 kDa enzyme comprised of a single polypeptide chain.[7] These assignments have been used as a starting point to address issues relating to the energetics and kinetics of substrate binding, domain reorientation upon ligand binding, and internal dynamics.[8] Recently we have also reported the near complete assignment of methyl ^1H and ^{13}C chemical shifts of Ile ($\delta 1$), Leu, and Val residues in the protein, using a series of experiments and a labeling scheme that we have found to be optimal for applications to high molecular weight proteins.[9]

With the chemical shift assignments of an important subset of the available NMR spins now in hand, we turn our attention to structural studies of MSG. In particular, our long-term goal is to establish whether useful structural information on a system of this size can be obtained from a limited set of NOEs involving backbone amides and side chain methyls and supplemented by dipolar couplings. To make full use of NOE data, it is clear that stereospecific assignments of Leu and Val methyls are a prerequisite,[10] and in the present work, we wish to obtain such assignments for as many of the 70 Leu and 46 Val residues (232 methyls) as possible. The large number of methyls and the significant size of the protein (correlation times of 37 and 45 ns in H_2O and D_2O, respectively) present serious challenges for the assignment.

We report here an approach which makes use of (i) the 10% ^{13}C-fractional labeling method of Wüthrich and co-workers[11,12] which has been so successful in applications involving small-to-medium sized proteins in the past and (ii) a quantitative *J* based strategy[13,14] for the measurement of $^3J_{C\gamma N}$ and $^3J_{C\gamma C'}$ couplings initially developed by the Bax group for the stereoassignment of Val methyls.[15,16] We present new methyl-TROSY[17,18] quantitative *J* experiments that exploit the cancellation of intra-methyl $^1H-^1H$ and $^1H-^{13}C$ dipolar interactions that would otherwise significantly degrade resolution and

(1) Pervushin, K.; Riek, R.; Wider, G.; Wüthrich, K. *Proc. Natl. Acad. Sci. U.S.A.* **1997**, *94*, 12366−12371.
(2) Pervushin, K.; Riek, R.; Wider, G.; Wüthrich, K. *J. Am. Chem. Soc.* **1998**, *120*, 6394−6400.
(3) Yang, D.; Kay, L. E. *J. Biomol. NMR* **1999**, *13*, 3−10.
(4) Pervushin, K. *Q. Rev. Biophys.* **2000**, *33*, 161−197.
(5) Yang, D.; Kay, L. E. *J. Am. Chem. Soc.* **1999**, *121*, 2571−2575.
(6) Konrat, R.; Yang, D.; Kay, L. E. *J. Biomol. NMR* **1999**, *15*, 309−313.
(7) Tugarinov, V.; Muhandiram, R.; Ayed, A.; Kay, L. E. *J. Am. Chem. Soc.* **2002**, *124*, 10025−10035.
(8) Tugarinov, V.; Kay, L. E. *J. Mol. Biol.* **2003**, *327*, 1121−1133.
(9) Tugarinov, V.; Kay, L. E. *J. Am. Chem. Soc.* **2003**, *125*, 13868−78.
(10) Hilty, C.; Wider, G.; Fernandez, C.; Wüthrich, K. *J. Biomol. NMR* **2003**, *27*, 377−82.
(11) Neri, D.; Szyperski, T.; Otting, G.; Senn, H.; Wüthrich, K. *Biochemistry* **1989**, *28*, 7510−7516.
(12) Szyperski, T.; Neri, D.; Leiting, B.; Otting, G.; Wüthrich, K. *J. Biomol. NMR* **1992**, *2*, 323−334.
(13) Bax, A.; Max, D.; Zax, D. *J. Am. Chem. Soc.* **1992**, *114*, 6923−6925.
(14) Bax, A.; Vuister, G. W.; Grzesiek, S.; Delaglio, F.; Wang, A. C.; Tschudin, R.; Zhu, G. *Methods Enzymol.* **1994**, *239*, 79−105.
(15) Vuister, G. W.; Wang, A. C.; Bax, A. *J. Am. Chem. Soc.* **1993**, *115*, 5334−5335.
(16) Grzesiek, S.; Vuister, G. W.; Bax, A. *J. Biomol. NMR* **1993**, *3*, 487−493.
(17) Tugarinov, V.; Hwang, P. M.; Ollerenshaw, J. E.; Kay, L. E. *J. Am. Chem. Soc.* **2003**, *125*, 10420−10428.
(18) Ollerenshaw, J. E.; Tugarinov, V.; Kay, L. E. *Magn. Reson. Chem.* **2003**, *41*, 843−852.

10.1021/ja048738u CCC: $27.50

sensitivity. A combination of these two approaches has provided stereospecific assignments for ~90% of the Val methyls in MSG, while ~80% of the Leu methyls in the protein have been assigned exclusively using the Neri method.[11] The two methodologies are shown to be complementary. For ~55% of the Val residues, data from both the fractional labeling and quantitative *J* approaches are available and both data sets predict the same stereoassignment. The remaining 30% of the Val stereoassignments are derived from data generated by only one of the two methods (~15% from each). Finally, $^3J_{C\gamma N}$ and $^3J_{C\gamma C'}$ couplings have been used to provide information about χ_1 rotamer averaging in valines,[15,16,19] and a significant correlation between χ_1 averaging established on the basis of these couplings and millisecond time scale side chain dynamics probed by methyl-TROSY relaxation dispersion experiments[20] is noted.

Materials and Methods

NMR Samples. A U-[^{2}H,^{15}N,^{13}C] Ileδ1-[$^{13}CH_3$], Leu,Val-[$^{13}CH_3$,$^{12}CD_3$] sample of MSG was prepared using D_2O-based minimal growth media with [^{13}C,^{2}H]-D-glucose as the main carbon source, described in detail previously.[9] 2-Keto-3,3-d_2-1,2,3,4-^{13}C-butyrate (120 mg) and 2-keto-3-methyl-d_3-3-d_1-1,2,3,4-^{13}C-butyrate (200 mg) were both added to 2 L of growth medium 1 h prior to induction, which led to the methyl labeling pattern indicated above (note that the labeling of the Leu and Val methyls is not stereospecific). A 0.9 mM sample was prepared in 92% H_2O/8% D_2O, 25 mM sodium phosphate, pH 7.1, 20 mM $MgCl_2$, 0.05% NaN_3, 0.1 mg/mL Pefabloc, and 5 mM DTT. A second MSG sample, U-[^{2}H,^{15}N,^{12}C] Ileδ1-[$^{13}CH_3$] Leu,Val-[$^{13}CH_3$,$^{12}CD_3$] MSG, with ^{13}C labeling restricted to the methyl positions indicated above was prepared as described elsewhere[21] using [^{12}C,^{2}H]-D-glucose as the main carbon source. In this case, 2-keto-3,3-d_2-4-^{13}C-butyrate (Ile δ1) and 2-keto-3-methyl-d_3-3-d_1-4-^{13}C-butyrate ([$^{13}CH_3$,$^{12}CD_3$] labeling of Leu, Val) were used. This sample (1.0 mM in protein) was prepared in 99% D_2O buffer containing 25 mM sodium phosphate, pH 7.1 (uncorrected), 20 mM $MgCl_2$, 0.05% NaN_3, 0.1 mg/mL Pefabloc, and 5 mM DTT. All biosynthetic precursors were obtained from Isotec (Miamisburg, OH) and quantitatively exchanged to ^{2}H at position 3 according to Gardner and Kay[22] and Goto et al..[23]

A fully protonated, fractionally ^{13}C-labeled (10% ^{13}C) sample of MSG was prepared in 1 L of H_2O-based minimal media with 10% [^{13}C]/90% [^{12}C]-D-glucose as the main carbon source. To eliminate potential overlap of Val methyl resonances with γ-CH_2 groups of Lys and γ2 methyls of Thr and Ile, unlabeled Ile, Thr, and Lys amino acids (400 mg each) were added to the growth medium 45 min prior to induction of protein overexpression.[24] The fractionally ^{13}C-labeled MSG preparation was purified as described earlier,[7] and a 0.9 mM sample, 99% D_2O, 25 mM sodium phosphate, pH 7.1 (uncorrected), 20 mM $MgCl_2$, 0.05% NaN_3, 0.1 mg/mL Pefabloc, and 5 mM DTT, was prepared.

NMR Spectroscopy. All NMR experiments were performed on an 800 MHz four-channel Varian Inova spectrometer operating at 37 °C and equipped with a room-temperature pulsed-field gradient triple resonance probe. Each of the 2D ZQ-SED (zero-quantum spin−echo difference), Figure 2, and MQ (multiple-quantum)-SED, Figure 3a, experiments for the measurement of $^3J_{C\gamma N}$ couplings were recorded in an interleaved manner (see below) on the U-[^{2}H,^{15}N,^{12}C] Ileδ1-[$^{13}CH_3$] Leu,Val-[$^{13}CH_3$,$^{12}CD_3$] MSG sample with (186, 768) complex points in the (^{13}C, ^{1}H) dimensions and (t_1, t_2) acquisition times of 76.7 ms and 64 ms. A relaxation delay of 1.1 s and a constant-time delay T of 80 ms were used in both experiments along with 72 scans/FID, giving rise to a total acquisition time of 18.5 h for each complete interleaved data set. 2D MQ-SED spectra for the measurement of $^3J_{C\gamma C'}$ couplings (pulse schemes of Figure 3b and Figure 1 of the Supporting Information) were acquired in an interleaved manner on the U-[^{2}H,^{15}N,^{13}C] Ileδ1-[$^{13}CH_3$], Leu,Val-[$^{13}CH_3$,$^{12}CD_3$] sample of MSG, using (124, 768) complex points in the (^{13}C, ^{1}H) dimensions, (t_1, t_2) acquisition times of (51 ms, 64 ms) and 80 transients/FID resulting in a total experimental time of 18 h for an interleaved matrix (relaxation delay of 1.5 s; constant-time delay T = 54 ms). ^{1}H−^{13}C CT-HSQC spectra[25,26] were recorded on the fully protonated, 10% fractionally ^{13}C-labeled sample of MSG (see above) with constant-time delays of 28 ms[25] ($1/^1J_{CC}$) and 42 ms,[27] and with (t_1, t_2) acquisition times of (27 ms, 64 ms) and (42 ms, 64 ms) in (^{13}C, ^{1}H) dimensions, respectively. 186 scans/FID were recorded, resulting in net experimental times of 16 and 25 h (relaxation delay of 1.3 s). NMR data sets were processed using NMRPipe/NMRDraw software[28] with peak intensities measured with the program PIPP.[29] NMR spectra were analyzed with NMRView[30] using the assignments of Leu and Val methyl groups obtained previously.[9]

Results and Discussion

Stereospecific Methyl Assignments in MSG via Fractional ^{13}C-Labeling. An elegant method for the stereospecific assignment of prochiral methyls of Leu and Val residues was proposed by the Wüthrich group over a decade ago based on fractional (10%) ^{13}C-labeling of proteins using a carbon source consisting of a 1:10 combination of ^{13}C-glucose/^{12}C-glucose.[11,12] The approach relies on the fact that the pro-R and directly bonded carbon ($C_{\gamma 1}$,C_β in Val and $C_{\delta 1}$,C_γ in Leu) derive from the same pyruvate molecule, while the pro-S methyl and the adjacent carbon originate from different pyruvates. As a consequence, with the ratio of ^{13}C- to ^{12}C-glucose indicated above, the probability of simultaneous incorporation of ^{13}C into the C_β(Val) or C_γ (Leu) and pro-R methyl carbon positions is 10 times higher than that for the corresponding labeling pattern involving the pro-S methyl carbon. It is possible, therefore, to distinguish in a straightforward manner between the pro-R and pro-S methyls based on the presence or absence of ^{13}C−^{13}C ^1J couplings between one of the diastereotopic methyls and the adjacent carbon using ^{1}H−^{13}C based correlation experiments. Applications of this methodology to relatively large proteins or protein complexes include the near complete stereospecific assignments of Leu, Val methyls in maltose binding protein[31] (42 kDa, 370 residues) and in the OmpX membrane protein in DHPC micelles[10] (approximately 60 kDa for the complex of lipid and protein, 148 residues). Our goal in the present work is to obtain such assignments for malate synthase G (82 kDa, 723 residues), a single polypeptide enzyme that includes 70 Leu and 46 Val residues.

Figure 1a illustrates a constant-time (CT, 28 ms) ^{1}H−^{13}C HSQC spectrum recorded on a 0.9 mM, 10% ^{13}C-labeled sample of MSG that has been used to obtain Leu, Val stereospecific assignments. A number of different CT delays were em-

(19) Chou, J. J.; Case, D. A.; Bax, A. *J. Am. Chem. Soc.* **2003**, *125*, 8959−8966.
(20) Korzhnev, D. M.; Klober, K.; Kanelis, V.; Tugarinov, V.; Kay, L. E. *J. Am. Chem. Soc.* **2004**, 126, 3964−3973.
(21) Tugarinov, V.; Kay, L. E. *J. Biomol. NMR* **2004**, *28*, 165−172.
(22) Gardner, K. H.; Kay, L. E. *J. Am. Chem. Soc.* **1997**, *119*, 7599−7600.
(23) Goto, N. K.; Gardner, K. H.; Mueller, G. A.; Willis, R. C.; Kay, L. E. *J. Biomol. NMR* **1999**, *13*, 369−374.
(24) Atreya, H. S.; Chary, K. V. *J. Biomol. NMR* **2001**, *19*, 267−272.
(25) Vuister, G. W.; Bax, A. *J. Magn. Reson.* **1992**, *98*, 428−435.
(26) Santoro, J.; King, G. C. *J. Magn. Reson.* **1992**, *97*, 202−207.
(27) Hu, W.; Zuiderweg, E. R. *J. Magn. Reson. B* **1996**, *113*, 70−75.
(28) Delaglio, F.; Grzesiek, S.; Vuister, G. W.; Zhu, G.; Pfeifer, J.; Bax, A. *J. Biomol. NMR* **1995**, *6*, 277−293.
(29) Garrett, D. S.; Powers, R.; Gronenborn, A. M.; Clore, G. M. *J. Magn. Reson.* **1991**, *95*, 214−220.
(30) Johnson, B. A.; Blevins, R. A. *J. Biomol. NMR* **1994**, *4*, 603−614.
(31) Gardner, K. H.; Zhang, X.; Gehring, K.; Kay, L. E. *J. Am. Chem. Soc.* **1998**, *120*, 11738−11748.

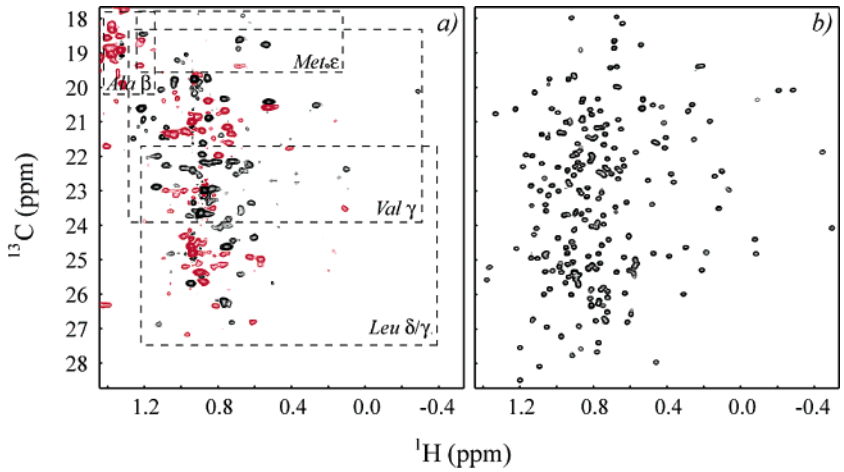

Figure 1. (a) Leu, Val methyl region of a ^{1}H−^{13}C CT-HSQC correlation spectrum[25,26] (800 MHz) recorded on a protonated, fractionally ^{13}C-labeled sample of MSG with selective "unlabeling" of Ile, Thr, and Lys residues[24] (see Materials and Methods). The data set was acquired with a constant-time period of 28 ms ($1/^{1}J_{CC}$). Negative cross-peaks are shown in red and correspond to $\gamma 1(\delta 1)$ methyls of Val(Leu); the negative cross-peaks in the upper left corner of the spectrum arise from alanine methyl groups, while several positive peaks in the same region and in the uppermost portion of the plot correspond to methyls of methionines. Total acquisition time of 16 h. (b) Leu, Val methyl region of a ^{1}H−^{13}C HMQC spectrum[34,35] (800 MHz) acquired on a U-[^{2}H,^{15}N,^{12}C] Ileδ1-[$^{13}CH_3$] Leu,Val-[$^{13}CH_3$,$^{12}CD_3$] sample of MSG (t_1 acquisition time of 105 ms) in 35 min.

ployed,[10,27] including $T = 28$ and 42 ms, but in practice, a delay of 28 ms proved to be the best compromise between sensitivity and resolution. Stereospecific assignments can be obtained directly by inspection of this spectrum, since correlations derived from ^{13}C methyls that are one-bond coupled to a ^{13}C partner are of opposite phase (red) relative to cross-peaks from isolated ^{13}C spins. Although the quality of the spectrum is rather marginal, stereospecific assignments for 58 Leu (83%) and 34 Val (76%) were obtained using this approach. The large number of assignments obtained reflects the fact that for each Leu/Val only one of the two expected methyl correlations must be observed in spectra, since the phase of the observed correlation automatically gives the stereoassignment, although independent stereospecific assignment of each methyl is of course preferred. 54% of Leu and 35% of Val methyls were stereospecifically assigned on the basis of observation of only a single correlation (the remaining assignments were made by observing correlations from both prochiral methyls). Stereospecific methyl assignments of the Leu residues are listed in the Supporting Information.

During the course of the assignments, we encountered a number of difficulties beyond those related to the issue of sensitivity. First, since the sample produced is fully protonated and our previous assignments were based on methyl protonated, highly deuterated preparations,[9] there are slight shifts in peak positions in the HSQC relative to those predicted from our assignment table due to two- and three-bond deuterium isotope effects (~0.3−0.4 ppm in ^{13}C).[32,33] In the present application involving 232 Leu, Val methyls, even small (and quite predictable) shifts can add complexity. Second, it is worth mentioning that cross-peaks derived from Thr and Ile γ2-methyls as well as γ-CH_2 groups of Lys can, in some cases, interfere with the correlations of interest. We have, therefore, simplified the methyl region by selective "unlabeling" of these amino acids[24] (see Materials and Methods), although cross-peaks from Ala β-methyls and possibly γ-methines of Leu can interfere with the analysis and cannot be eliminated from spectra. Both the large number of methyls and the high molecular weight of the system pose serious challenges for stereospecific assignments. We have therefore turned to a combination of both the biosynthetic strategy described above and a methyl-TROSY[17,18]-based quantitative J approach[14] for Val, to maximize the number of residues for which such assignments could be obtained.

Merging Methyl-TROSY and Quantitative *J* Spectroscopy. Figure 1b illustrates a region from the ^{1}H−^{13}C HMQC[34,35] correlation map recorded on a U-[^{2}H,^{15}N,^{12}C] Ileδ1-[$^{13}CH_3$], Leu,Val-[$^{13}CH_3$,$^{12}CD_3$] sample of MSG (D_2O), and it is quite clear from a comparison of the data sets of Figure 1a,b that there are significant improvements both in resolution and in sensitivity that can be obtained when suitable labeling and the appropriate pulse scheme is used.[21] Our goal here is to exploit the high quality of the data set illustrated in Figure 1b and to develop a set of methyl-TROSY, quantitative J based experiments to quantify $^{3}J_{C\gamma N}$ and $^{3}J_{C\gamma C'}$ couplings in Val residues. Together, this pair of couplings is used to supplement stereospecific assignments of Val residues from the fractionally ^{13}C-labeled sample. In addition, such couplings can also used to probe side chain dynamics,[19,36] as described below. Regrettably, a similar set of experiments is not possible for Leu residues in the case of MSG for reasons that are listed below.

Before we proceed with a description of the quantitative J based pulse schemes that have been developed, it is worthwhile to briefly summarize the main features of methyl-TROSY spectroscopy that are germane for the present application. In a series of publications we have emphasized that the benefits of HMQC relative to HSQC derive from the fact that one of the two magnetization pathways in the HMQC scheme, and the only path that contributes to observed correlations in applications to large proteins such as MSG, involves coherences that relax slowly throughout the sequence.[17,18] Particularly important for the applications considered here is that, for an isolated methyl group tumbling in the macromolecular limit and assuming

(32) Venters, R. A.; Farmer, B. T.; Fierke, C. A.; Spicer, L. D. *J. Mol. Biol.* **1996**, *264*, 1101−1116.
(33) Gardner, K. H.; Rosen, M. K.; Kay, L. E. *Biochemistry* **1997**, *36*, 1389−1401.
(34) Mueller, L. *J. Am. Chem. Soc.* **1979**, *101*, 4481−4484.
(35) Bax, A.; Griffey, R. H.; Hawkings, B. L. *J. Magn. Reson.* **1983**, *55*, 301−315.
(36) Millet, O.; Mittermaier, A.; Baker, D.; Kay, L. E. *J. Mol. Biol.* **2003**, *329*, 551−563.

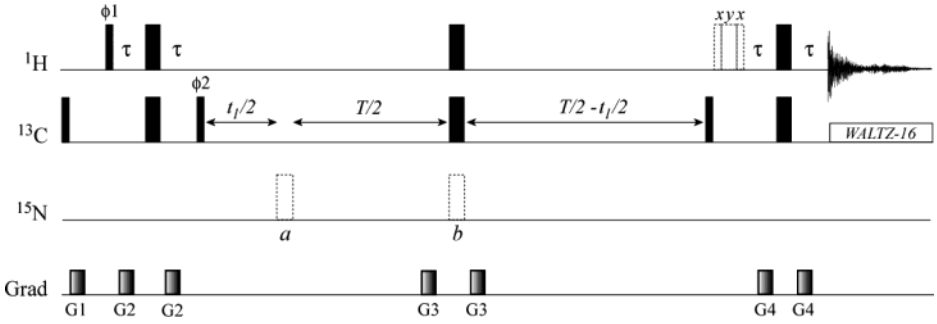

Figure 2. ZQ-SED pulse scheme for the measurement of $^3J_{C\gamma N}$ couplings in U-[^{2}H,^{15}N,^{12}C] Ileδ1-[$^{13}CH_3$], Leu,Val-[$^{13}CH_3$,$^{12}CD_3$] labeled samples in D_2O. (Note that ^{13}C-labeling is restricted to the methyl positions only.) Narrow (wide) pulses are applied with flip angles of 90° (180°) along the *x*-axis, unless indicated otherwise. The ^{1}H pulse shown with dashed lines is of the composite variety, $90°_x-180°_y-90°_x$.[49] rf pulses are centered at 0.7, 23, and 119 ppm for ^{1}H, ^{13}C, and ^{15}N, respectively. All pulses are applied at the highest field possible, with ^{13}C decoupling[50] during acquisition achieved using a 2.5 kHz field. $\tau = 1.8$ ms, with T set to approximately $2/R_{2,ZQ}$, where $R_{2,ZQ}$ is the relaxation rate of the slowly decaying ZQ element (L2, see text), $T = 80$ ms in the application to MSG. The phase cycle is as follows: $\phi1 = -y,-x$; $\phi2 = x,y,-x,-y$; rec $= 2(x),2(-x)$. Quadrature detection in F_1 is achieved by recording two separate FIDS for each t_1 point, with and without the ^{1}H composite 180° pulse shown with dashed lines.[37] The resulting data sets are manipulated according to the enhanced sensitivity protocol[40,51] to obtain pure absorptive line shapes. A pair of subspectra are recorded in an interleaved manner with (*i*) the ^{15}N 180° pulse at position *a* and with (*ii*) the ^{15}N 180° pulse at position *b*. Values of $^3J_{C\gamma N}$ couplings are obtained from the relation, $(I_a - I_b)/I_a = 1 - \cos(\pi^3 J_{C\gamma N} T)$, where I_a and I_b are peak intensities in the two separate subspectra with the ^{15}N 180° pulse applied at *a* or *b*, respectively (see text). The durations and strengths of the pulsed field gradients (applied along the *z*-axis) are as follows: G1 = (1.0 ms, 15 G/cm), G = (0.8 ms, 7.5 G/cm), G3 = (0.6 ms, 12 G/cm), G4 = (1.0 ms, −5 G/cm).

infinitely fast methyl rotation, the slowly relaxing multiple-quantum (MQ) elements decay in a manner that is independent of intra-methyl ^{1}H−^{1}H and ^{1}H−^{13}C dipolar fields.[17] It is instructive to write the ^{1}H−^{13}C MQ coherences of a methyl group, I_xC_x (I_j is the $j = \{x,y,z\}$ component of magnetization for spin I, I = ^{1}H, C = ^{13}C), in terms of components L1, L2, and L3 that separate the coherences on the basis of their different relaxation properties (i.e., fast vs slow). We write I_xC_x as $\Sigma_q I_{x,q}C_x$, where $q = \{1,2,3\}$ is an index which distinguishes each of the methyl protons, $I_{x,1}C_x = L1 + L2 + L3$, with $L1 = I_{x,1}C_x$ ($|\alpha\alpha><\alpha\alpha|$)^{2,3}, $L2 = I_{x,1}C_x$ ($|\alpha\beta><\alpha\beta| + |\beta\alpha><\beta\alpha|$)^{2,3}, $L3 = I_{x,1}C_x$ ($|\beta\beta><\beta\beta|$)^{2,3}, and |st> are spin states of methyl protons 2,3. Similar relations hold for $I_{x,2}C_x$ and $I_{x,3}C_x$. Coherences L1, L3 are part of the "fast relaxing pathway"and decay with time constants on the order of a few milliseconds for proteins the size of MSG.[17] In contrast, L2 is part of the slowly decaying path and relaxes predominantly from contributions involving external deuteron and proton spins; these contributions can be minimized by recording zero-quantum (ZQ) data sets, as discussed recently.[37] Only coherences described by L2 will be important in what follows.

In contrast to the HMQC scheme which sequesters fast and slowly relaxing coherences throughout the sequence, the HSQC experiment interconverts both fast and slowly relaxing elements which significantly compromises the resultant sensitivity.[17] Although HMQC spectra of high intensity and resolution can be recorded on large proteins, it is critical that samples be prepared that fully take advantage of the potential of the experiment. In particular, high levels of deuteration are essential. The high proton density in protonated samples leads to spin-flips involving external protons that would seriously undermine the TROSY effect,[21] much like in applications involving backbone amide ^{15}N, ^{1}HN spin systems.[38] In addition, homonuclear scalar couplings involving methyl and side chain protons would degrade the sensitivity of the experiment still further. We have recently shown that methyl-TROSY experiments can be optimally recorded using U-[^{2}H,^{15}N] Ileδ1-[$^{13}CH_3$], Leu,Val-[$^{13}CH_3$,$^{12}CD_3$] preparations.[21] Applications that measure $^3J_{C\gamma C'}$ scalar couplings require uniform ^{13}C-labeling, since it is currently not feasible to easily produce samples with ^{13}C enrichment confined to methyl and carbonyl positions only. We have, therefore, used a sample with the labeling pattern indicated above (i.e., Ileδ1-[$^{13}CH_3$], Leu,Val-[$^{13}CH_3$,$^{12}CD_3$]), with uniform ^{13}C-labeling at all nonmethyl positions for measurement of ^{13}C−^{13}C couplings. Since a sample of this type in H_2O was available from our previous work involving Ile, Leu, Val methyl assignments,[9] it was used to measure $^3J_{C\gamma C'}$ (see below). Our preference is to measure $^3J_{C\gamma N}$ coupling constants using samples of the type described above (Leu,Val-[$^{13}CH_3$,$^{12}CD_3$]) dissolved in D_2O solvent, with ^{13}C-labeling restricted to methyl positions in the protein. Replacement of amide protons with deuterons helps minimize external relaxation sources, while limiting ^{13}C-labeling to methyl sites ensures that experiments can be optimized with respect to the relaxation properties of the participating spins, without the need to refocus one-bond ^{13}C−^{13}C couplings. Sensitivity issues are particularly acute for measurement of $^3J_{C\gamma N}$ in large proteins, since these couplings are typically smaller than 2.5 Hz[14,19,39] and any improvements in experiment design are important.

Measurement of $^3J_{C\gamma N}$ and $^3J_{C\gamma C'}$ for Valine Residues in MSG Using Zero-Quantum and Multiple-Quantum Spectroscopy. The methods of quantitative *J* spectroscopy developed by Bax and co-workers for the measurement of scalar couplings in moderately sized proteins[14] can be easily modified for applications to large molecules. For proteins with molecular weights less than approximately 30−40 kDa, $^3J_{C\gamma N}$ and $^3J_{C\gamma C'}$ scalar couplings involving γ-methyls of Val are commonly measured using CT-HSQC-type pulse schemes.[25,26] Applications involving larger proteins would clearly benefit from MQ-[17] or ZQ[37]-based sequences, as described above.

Figure 2 shows the HZQC (zero-quantum) quantitative *J* scheme for the measurement of $^3J_{C\gamma N}$ in high molecular weight systems in D_2O with ^{13}C-labeling restricted to methyl groups (Leu-,Val-[$^{13}CH_3$,$^{12}CD_3$]). Zero-quantum ^{1}H−^{13}C coherences

(37) Tugarinov, V.; Sprangers, R.; Kay, L. E. *J. Am. Chem. Soc.* **2004**, *126*, 4921−4925.
(38) Wider, G.; Wüthrich, K. *Curr. Opin. Struct. Biol.* **1999**, *9*, 594−601.
(39) Perez, C.; Lohr, F.; Rüterjans, H.; Schmidt, J. M. *J. Am. Chem. Soc.* **2002**, *123*, 7081−7093.

evolve for a constant-time period of duration T, during which time net evolution due to $^3J_{C\gamma N}$ either does (^{15}N 180° pulse at position *b*) or does not occur (position *a*). Following Bax and co-workers,[15] the ratio of cross-peak intensities measured in spectra recorded with the ^{15}N 180° pulse in positions *b* (I_b) and *a* (I_a) is given by $I_b/I_a = \cos(\pi^3 J_{C\gamma N}T)\cos(\pi^4 J_{H\gamma N}T)$; assuming $^4J_{H\gamma N} \approx 0$ (see below), $^3J_{C\gamma N}$ can be calculated directly from I_b/I_a. A number of features of this experiment are worthy of comment. First, only ^{1}H−^{13}C zero-quantum coherences are selected as opposed to both zero- and double-quantum elements in HMQC versions. In the absence of relaxation, this translates into a factor of 2 sensitivity loss relative to HMQC-based approaches. Some of the sensitivity loss ($\sqrt{2}$) can be recovered by recording both cosine and sine t_1 modulated components in each scan using an "enhanced sensitivity scheme",[40] where two separate FIDs are obtained for each t_1 point, one with and a second without the composite ^{1}H 180° pulse immediately before the final 2τ element.[37] In this regard, it is noteworthy that we have been unable to develop a comparable enhanced sensitivity scheme for the HMQC experiment, since all versions include additional ^{1}H 90° pulses which lead to a mixing of fast and slowly relaxing proton transitions and subsequent sensitivity and resolution losses. There is a second important factor of enhancement, deriving from the differences in decay rates of ^{1}H−^{13}C double- and zero-quantum methyl coherences. We have recently shown that, for MSG labeled as described above, $R_{DQ}/R_{ZQ} \approx 1.8$, where R_{DQ} and R_{ZQ} are the relaxation rates for the slowly relaxing transverse double- and zero-quantum components[37] (the fast relaxing components make essentially no contribution to HMQC or HZQC spectra for molecules the size of MSG). Using a value of $T = 80$ ms, a relaxation rate, $^1/_2(R_{DQ} + R_{ZQ}) = 25$ s^{-1} for multiple quantum elements,[37] and $R_{ZQ} = 18$ s^{-1} (correlation time of 45 ns in D_2O) and taking into account that the HMQC scheme is $\sqrt{2}$ more sensitive than the enhanced HZQC experiment in the absence of relaxation, a gain in sensitivity of approximately 25% is predicted for correlations in the HZQC relative to the HMQC experiment. We have observed exactly this gain, on average, in a comparison of data sets recorded on MSG which make use of the sequences of Figures 2 and 3a (HMQC scheme for measuring $^3J_{C\gamma N}$, see below).

It is worth noting that the HZQC map described above must be recorded on samples with ^{13}C-labeling restricted to one of the two methyl positions. In experiments recorded on uniformly ^{13}C-labeled samples, the pair of simultaneous ^{1}H and ^{13}C 180° pulses applied during the constant-time T element would lead to intensity modulation from a series of ^{1}H$_m$−^{13}C scalar couplings including, $^2J_{H_m,C\beta}$, $^3J_{H_m,C\alpha}$, $^3J_{H_m,C_m}$, and $^4J_{H_m,C'}$. Note that the coherence of interest, L2, does not evolve due to $^1J_{H_m,C_m}$. Three-bond ^{1}H$_m$−^{13}C couplings can be as large as 4−5 Hz,[41,42] and two-bond couplings are of similar magnitude but opposite sign.[42] It is thus quite clear that for the long values of T required to evolve the (small) $^3J_{C\gamma N}$ coupling there would be substantial losses in sensitivity (2−3-fold) from the passive ^{1}H$_m$−^{13}C couplings in applications using uniformly ^{13}C-labeled samples or even using samples labeled with ^{13}C only at both of the methyl positions.

Since it is not possible to easily refocus ^{1}H$_m$−^{13}C couplings in the context of an HZQC experiment, and since experiments for measuring $^3J_{C\gamma C'}$ couplings are carried out on samples that are uniformly ^{13}C-labeled (see above), such experiments must employ HMQC schemes. These sequences refocus the two-, three-, and four-bond ^{1}H$_m$−^{13}C scalar couplings described above and can therefore be used with uniformly ^{13}C-labeled samples (or ^{13}C-methyl-labeled samples where $^3J_{C\gamma N}$ is measured). Figures 3a and b show the HMQC-based quantitative J pulse schemes that have been developed for measuring $^3J_{C\gamma N}$ and $^3J_{C\gamma C'}$, respectively. As with the ZQ scheme, a pair of data sets are recorded with evolution of $^{13}C_\gamma$ magnetization due to the ^3J of interest for a time T (dashed pulses applied at position *b* in either sequence) or where net evolution is refocused (dashed pulses applied at *a*) and the value of ^3J calculated directly from $I_b/I_a = \cos(\pi^3 JT)$. The experiments are optimized for samples in H_2O by ensuring that water magnetization is along the *z*-axis throughout the sequence. Preserving water magnetization is particularly important in applications involving very high molecular weight proteins,[43,44] where exchange between water and labile hydrogens followed by magnetization transfer can significantly attenuate even those correlations that derive from nonlabile sites (such as methyl groups). For example, in the case of maltose binding protein (correlation time 17 ns in H_2O, pH 7.2, 37 °C), dephasing of water at the start of a ^{1}H−^{13}C correlation experiment leads to a decrease in the intensity of methyl correlations by 10%, on average. In the case of MSG (correlation time of 37 ns in H_2O, pH 7.1, 37 °C), dephasing results in a larger decrease in sensitivity, ∼20−25%.

Figure 4a shows a difference data set, obtained by subtracting a pair of maps recorded with the pulse scheme of Figure 2, with the ^{15}N 180° pulse in either position *a* or *b*. Correlations in the difference spectrum are restricted to Val residues, with 41 of the 46 valines contributing at least one peak. The corresponding spin−echo difference map (SED) obtained from data sets measured using the sequence of Figure 3b is shown in Figure 4b, with correlations from 37 Val residues observed. In general, cross-peaks from only one of the two possible diastereotopic methyls are found in the difference maps, except for a number of cases that very likely involve rotameric averaging.

As described above, in the case of the ZQ-SED experiment, the spin−echo difference intensity is modulated by the product $\cos(\pi^3 J_{C\gamma N}T)\cos(\pi^4 J_{H\gamma N}T)$. Although ^4J values are likely to be negligible, it is important to confirm that $^4J_{H\gamma N} \approx 0$, an assumption that has been used in the quantification of cross-peak intensities in ZQ data sets. Figure 5a plots the correlation between $^3J_{C\gamma N}$ couplings measured using the HZQC and HMQC experiments. Recall that the MQ scheme refocuses evolution from $^4J_{H\gamma N}$, while the ZQ scheme does not. The pairwise rmsd between $^3J_{C\gamma N}$ values is 0.12 Hz which is smaller than the errors in the measurements (average errors are 0.21 and 0.25 Hz for ZQ-SED and MQ-SED experiments, respectively). It is clear that the contributions from $^4J_{H\gamma N}$ in the ZQ experiment are small and will not interfere with stereospecific assignments. Figure 5a shows that the measured $^3J_{C\gamma N}$ couplings range from 0.7 to 2.2 Hz with values close to 2 Hz corresponding to a trans configuration of the C_β−C_γ and C_α−N bonds, while the gauche configuration gives a coupling on the order of 0.5 Hz.[19,39] For

(40) Cavanagh, J.; Rance, M. *Annu. Rep. NMR Spectrosc.* **1993**, *27*, 1−58.
(41) Wasylishen, R.; Schafer, T. *Can. J. Chem.* **1972**, *50*, 3686−3692.
(42) Nelson, J. H. *Nuclear Magnetic Resonance Spectroscopy*; Prentice Hall: NJ, 2003.
(43) Grzesiek, S.; Bax, A. *J. Am. Chem. Soc.* **1993**, *115*, 12593−12594.
(44) Riek, R.; Fiaux, J.; Bertelsen, E. B.; Horwich, A. L.; Wüthrich, K. *J. Am. Chem. Soc.* **2002**, *124*, 12144−12153.

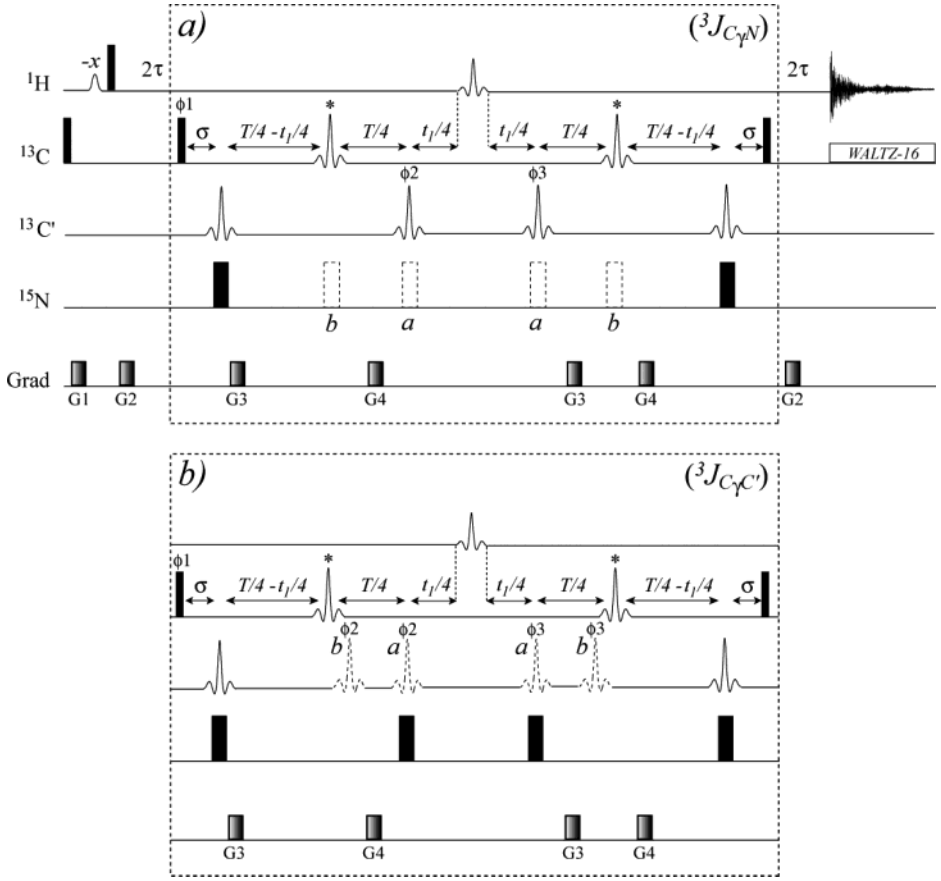

Figure 3. MQ-SED pulse schemes for the measurement of $^3J_{C\gamma N}$ (a) and $^3J_{C\gamma C'}$ (b) couplings in U-[^{2}H,^{15}N,^{13}C] Ileδ1-[$^{13}CH_3$], Leu,Val-[$^{13}CH_3$,$^{12}CD_3$] labeled samples in H_2O. All rectangular ^{1}H, ^{13}C, and ^{15}N pulses are applied with the highest available power, with ^{13}C WALTZ-16 decoupling[50] achieved using a 2.5 kHz field. The carriers are positioned at 4.7 (water resonance), 23, and 119 ppm for ^{1}H, ^{13}C, and ^{15}N, respectively. The first shaped ^{1}H pulse is a 90° water-selective rectangular pulse of ~1.5 ms duration, while the ^{1}H 180° pulse in the middle of constant-time delay T has a RE-BURP profile[52] (~1.5 ms duration at 800 MHz, centered at 0 ppm by phase modulation of the carrier.[53,54] This pulse covers the range of methyl ^{1}H chemical shifts while leaving the water magnetization unperturbed). ^{13}C shaped (RE-BURP) pulses marked with * (180°) are applied on resonance and are 300 μs in length (800 MHz). Carbonyl 180° shaped (RE-BURP, 300 μs) pulses are applied at 178 ppm by phase modulation of the carrier. The delay τ is set to 1.8 ms with $4\sigma + T$ a multiple of $1/^1J_{CC}$, σ = half the duration of the methyl-selective ^{1}H RE-BURP pulse in the middle of the constant-time period, and T the duration during which the ^3J coupling of interest is allowed to evolve (pulses at *b*, see below and text); T = 54 ms in the present application. The phase cycle employed: $\phi1 = x,-x$; $\phi2 = 2(x),2(-x)$; $\phi3 = 4(x),4(-x)$; rec = $x,-x$. Quadrature detection in F_1 is achieved by States-TPPI[55] of phase $\phi1$. For the measurement of $^3J_{C\gamma N}$ ($^3J_{C\gamma C'}$) couplings, two subspectra are recorded in an interleaved manner with ^{15}N (^{13}C′) pulses applied at positions *a* and *b*. The values of ^3J are calculated from the ratios $(I_a - I_b)/I_a$ as described in the text. The durations and strengths of the pulsed field gradients applied along the *z*-axis are as follows: G1 = (1.0 ms, 15 G/cm), G2 = (0.8 ms, 7.5 G/cm), G3 = (0.1 ms, 12 G/cm), G4 = (0.3 ms, −25 G/cm).

MSG, $^3J_{C\gamma N}$ values less than approximately 1 Hz could not be measured, in general.

Figure 5b shows a histogram of $^3J_{C\gamma C'}$ scalar couplings obtained using the pulse scheme of Figure 3b. $^3J_{C\gamma C'}$ values range from approximately 4 Hz, corresponding to $C_\beta - C_\gamma$ and $C_\alpha - C'$ bonds in the trans configuration, to ~1 Hz, indicative of a gauche configuration.[15,16,19,39] As a check on the measured $^3J_{C\gamma C'}$ values, we have written a second sequence that refocuses $^1H_m - ^{13}C$ couplings differently than the first (see Supporting Information) and recorded an additional set of couplings. The pairwise rmsd between values from the two experiments is 0.2 Hz (Supporting Information), lending confidence in the reported $^3J_{C\gamma C'}$ values.

Measured values of $^3J_{C\gamma N}$ and $^3J_{C\gamma C'}$ couplings are affected by a number of systematic errors[16] resulting primarily from (i) incomplete isotopic enrichment in samples (the precursors used were ≥97% in ^{15}N or ^{13}C), (ii) incomplete inversion of magnetization by ^{15}N or ^{13}C′ 180° pulses (inversion levels of 98 and 96% have been measured for ^{15}N and ^{13}C′ pulses, respectively), and (iii) differential relaxation between transverse C_γ magnetization that is in-phase or antiphase with respect to coupled ^{15}N ($^3J_{C\gamma N}$) or ^{13}C′ ($^3J_{C\gamma C'}$) spins. Each of the three effects leads to a (small) decrease in the measured values of the couplings that is well within the average standard errors in $^3J_{C\gamma N}$ (13%) and $^3J_{C\gamma C'}$ (8%) values.

Stereospecific Assignments, Rotameric States, and Dynamics of Val Side Chains in MSG. Values of $^3J_{C\gamma N}$ and $^3J_{C\gamma C'}$ couplings measured for the pair of methyls of a given Val can provide unambiguous stereospecific assignments provided that the measured J couplings are consistent with a single, canonical ($\chi_1 = \pm 60°, 180°$) rotameric state.[14,15] It is noteworthy that a similar approach based on measurement of ^3J values is unlikely to be useful for providing stereospecific assignments of Leu residues in high molecular weight proteins. In principle, measurement of $^3J_{C\delta C\alpha}$ and $^3J_{C\delta H\beta}$ couplings would be sufficient for such assignments if the H_β protons were stereospecifically assigned in advance.[14] However, as discussed above, the application of quantitative J based experiments to high molecular weight proteins benefits tremendously from high levels of deuteration, conflicting with the requirements of protonation for

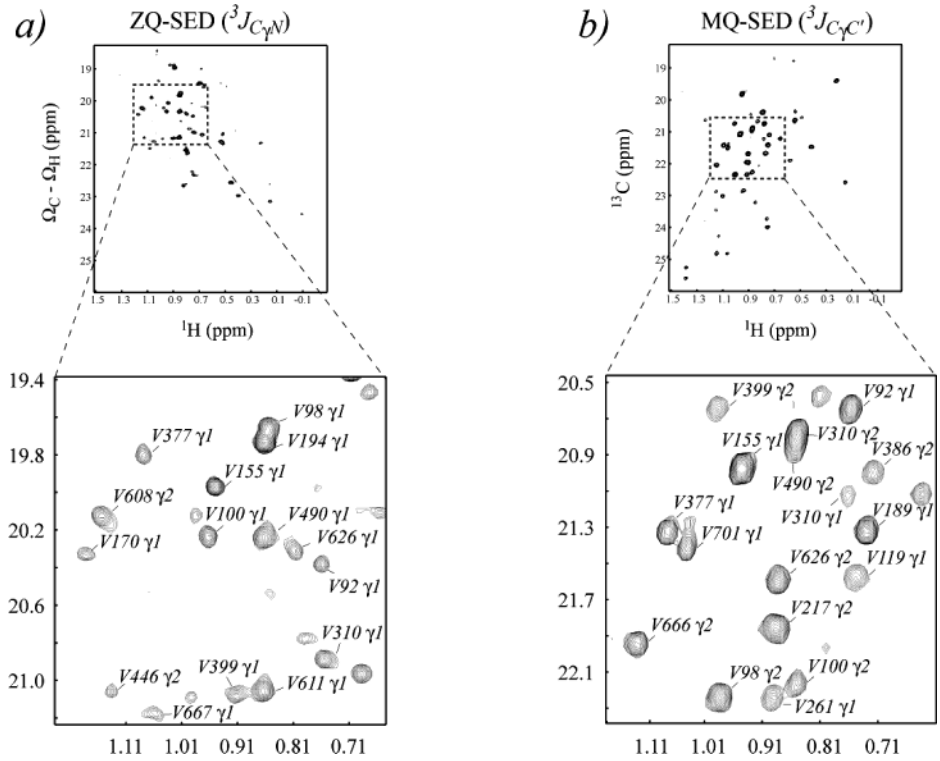

Figure 4. ZQ and MQ spin−echo difference (SED) spectra used to quantify $^3J_{C\gamma N}$ and $^3J_{C\gamma C'}$ coupling constants in Val side chains of MSG. (a) ZQ-SED spectrum of U-[^{2}H,^{15}N,^{12}C] Ileδ1-[$^{13}CH_3$], Leu,Val-[$^{13}CH_3$,$^{12}CD_3$]-MSG (D_2O) acquired with the pulse sequence of Figure 2. The resonances appearing in the spectrum correspond to large (usually $>\sim$1.5 Hz) $^3J_{C\gamma N}$ couplings. The correlations in the ZQ-SED spectrum appear at frequencies of $\Omega_C-\Omega_H$ in the F_1 dimension, where $\Omega_{C,H}$ is the offset from the C,H carrier and are recast in terms of ^{13}C ppm values. (b) MQ-SED spectrum recorded on a U-[^{2}H,^{15}N,^{13}C] Ileδ1-[$^{13}CH_3$], Leu,Val-[$^{13}CH_3$,$^{12}CD_3$]-MSG sample, H_2O, acquired with the pulse sequence of Figure 3b. The resonances appearing in the spectrum correspond to large (usually $>\sim$1.0 Hz) $^3J_{C\gamma C'}$ values. Regions shown in dashed boxes are enlarged below, and peaks labeled with the stereospecific assignments were obtained from either the combination of measured $^3J_{C\gamma N}$ and $^3J_{C\gamma C'}$ couplings or the method of fractional ^{13}C-labeling.[11,12]

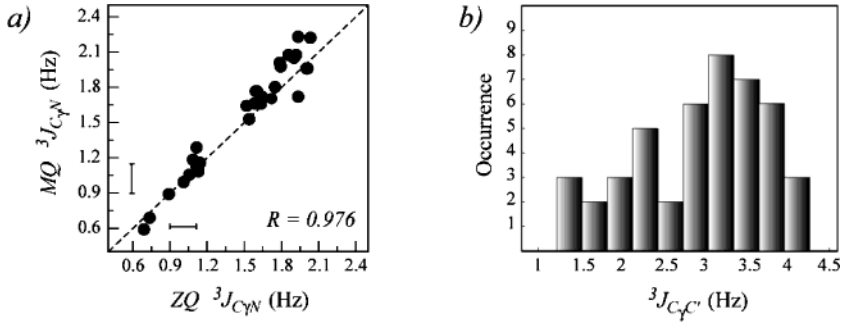

Figure 5. (a) Correlation plot of $^3J_{C\gamma N}$ couplings from Val side chains in MSG measured from ZQ-SED (*x*-axis) and MQ-SED (*y*-axis) spectra. 28 values of $^3J_{C\gamma N}$ obtained from completely separated resonances in both ZQ and MQ spectra were selected for comparison. The bars drawn along the *x* and *y* axes near the origin of the plot correspond to average standard errors in the measurements, estimated from root mean squared differences of peak intensities, $D = I_a - I_b$, of Leu and Ile resonances and subsequently propagated to errors in $^3J_{C\gamma N}$ according to Vuister et al.[15] (b) Histogram of $^3J_{C\gamma C'}$ couplings of Val side chains of MSG obtained with the MQ-SED experiment, Figure 3b.

the measurement of $^3J_{C\delta H\beta}$ couplings. It seems unlikely that Leu H_β shifts could be assigned in large systems such as MSG in any case. We have therefore relied exclusively on the 10% ^{13}C-labeling strategy for the stereospecific assignment of Leu methyl groups.

Using a qualitative approach in which couplings are classified as large, small, or averaged (for example, large $> \sim$3 Hz, small $< \sim$1 Hz for $^3J_{C\gamma C'}$), we have been able to stereoassign and obtain approximate χ_1 values for 31 Val methyls, Table 1. For those valines where rotameric averaging precludes unambiguous stereospecific assignments from *J* coupling data, the method of Wüthrich and co-workers[11,12] employing fractional ^{13}C-labeling was used. It is clear from Table 1 that these two approaches are complementary; 34 methyls were stereoassigned using fractional labeling exclusively (31 methyls from ^3J values), while a combination of both approaches provided stereoassignments for 41 Val methyls of MSG (out of 45 assigned Val, corresponding to 91%).

The dominant rotameric states derived from *J* coupling data are in excellent agreement with χ_1 torsion angles obtained from the X-ray structure of the glyoxylate-Mg^{2+}-bound form of the protein.[45] (In Table 1, χ_1 angles close to $\pm$180° correspond to trans and those close to +60°(−60°) correspond to gauche$^+$-(gauche$^-$) staggered configurations.) The only discrepancy is observed for V119 where the gauche$^-$ configuration derived from $^3J_{C\gamma N}$ and $^3J_{C\gamma C'}$ values is in disagreement with the χ_1 angle

Table 1. $^3J_{C\gamma C'}$, $^3J_{C\gamma N}$ Values Stereospecific Assignments and Rotameric States of the Valine Side Chains in Malate Synthase G

	$C^{\gamma 1}$ [a]				$C^{\gamma 2}$ [a]				Rotameric state	
	$^1H\delta$	$^{13}C\delta$	$^3J_{C\gamma N}$	$^3J_{C\gamma C'}$	$^1H\delta$	$^{13}C\delta$	$^3J_{C\gamma N}$	$^3J_{C\gamma C'}$	NMR[b]	χ_1(°)[c]
V20	0.44	21.51	1.96 ± 0.18	< 1.4	0.72	23.88	< 1.0	3.77 ± 0.19	t	176.7
V24	0.51	20.53	[d]	[d]	0.12	22.49	< 1.2	3.59 ± 0.20	t	-173.7
V43	0.64	20.85	2.03 ± 0.18	< 1.6	1.02	24.73	< 1.5[d]	> 3.0[d]	t	173.3
V75	0.79	21.95	2.23 ± 0.17[d]	< 1.0[d]	0.80	20.58	< 1.2	3.63 ± 0.20	t	-179.5
V92[f]	0.75	20.66	0.89 ± 0.35	2.91 ± 0.24	0.67	18.61	< 1.2	1.48 ± 0.41	g^-	-49.2
V98	0.84	20.28	1.77 ± 0.20	< 1.4	0.97	22.24	0.59 ± 0.45	3.08 ± 0.22	t	168.2
V100[f]	0.94	21.25	1.80 ± 0.20[d]	< 1.5[d]	0.84	22.16	< 1.1	2.76 ± 0.25	t	167.8
V118	0.21	19.34	1.66 ± 0.19[e]	< 1.5	-0.86	17.61	< 1.5[e]	3.73 ± 0.19	t	-173.9
V119[f]	0.72	21.58	< 1.1	2.56 ± 0.26	0.67	18.79	< 1.2	< 1.3	g^-	70.9
V155[g]	0.93	20.99	1.16 ± 0.29	2.21 ± 0.30	0.92	19.72	0.69 ± 0.41	2.10 ± 0.31	-	-[i]
V166	0.82	21.11	2.27 ± 0.16	< 1.9	0.91	22.72	< 1.3	4.12 ± 0.18	t	167.8
V170	1.16	22.23	1.96 ± 0.18	< 2.0	1.36	25.49	< 1.6	4.26 ± 0.17	t	179.5
V188[f]	0.40	21.69	1.66 ± 0.21	< 1.7	0.73	23.61	< 1.1	2.80 ± 0.24	t	178.9
V189[f]	0.72	21.32	< 1.1	2.89 ± 0.24	0.52	18.70	< 0.8	1.64 ± 0.38	g^-	-48.6
V193	0.69	19.36	2.01 ± 0.18	< 1.3	0.19	19.32	< 1.1	3.40 ± 0.21	t	-168.9
V194	0.85	20.39	1.76 ± 0.20	< 0.9	0.76	20.30	0.59 ± 0.43	3.27 ± 0.22	t	169.5[h]
V217	0.78	21.92	~ 1.7[d]	< 1.0[d]	0.87	21.90	< 0.6[d]	~3.3[d]	t	164.2
V259	0.65	19.92	> 1.5[d]	< 1.7[d]	0.63	21.12	< 1.1	3.64 ± 0.20	t	-179.9
V261	0.88	22.23	< 0.9	3.17 ± 0.24	0.91	20.91	< 1.0	< 1.1	g^-	-59.0
V275[f]	0.82	23.10	1.09 ± 0.30	2.45 ± 0.27	0.77	21.34	[d]	[d]	-	138.1
V278[f]	0.40	20.94	1.02 ± 0.32	1.27 ± 0.29	0.62	18.05	< 2.0	< 3.0	-	-55.3
V310	0.73	21.11	1.64 ± 0.21	1.22 ± 0.47	0.84	20.83	[d]	[d]	t	-179.4[h]
V348	0.14	20.91	1.53 ± 0.23	< 1.5	0.39	21.36	< 1.0	3.28 ± 0.21	t	166.0
V365	-0.11	20.29	1.97 ± 0.16[e]	< 2.0	0.55	21.80	< 1.3	3.85 ± 0.19	t	169.4
V377[g]	1.06	21.33	1.02 ± 0.32	2.29 ± 0.29	1.20	20.52	< 1.2	1.99 ± 0.33	-	-[i]
V386	0.65	19.34	1.98 ± 0.18	< 1.9	0.71	21.00	< 1.1	3.40 ± 0.21	t	177.7
V399	0.90	21.88	2.19 ± 0.17	< 1.0	0.97	20.61	< 1.2	3.85 ± 0.19	t	179.8
V446[f]	0.96	21.23	~1.3[d,e]	< 1.2[d]	1.12	22.78	1.29 ± 0.26	2.20 ± 0.29	-	48.1
V464	0.46	20.46	< 1.1	3.29 ± 0.21	0.65	17.88	< 1.5	< 2.0	g^-	-52.4
V490	0.89	19.61	~ 1.8[d]	< 1.5[d]	0.85	20.91	[d]	[d]	t	177.5
V535	1.12	24.84	< 1.8	3.80 ± 0.19	0.90	17.91	< 1.5	< 2.0	g^-	-68.8
V553[f]	1.07	22.91	1.1 ± 0.23[e]	2.98 ± 0.23	1.10	20.11	< 1.0	< 1.3	g^-	-48.7
V581[f]	0.50	20.55	[d]	[d]	0.51	20.26	1.13 ± 0.29	1.56 ± 0.39	-	72.8
V607[f]	1.01	23.06	< 1.4	1.94 ± 0.33	1.11	26.63	< 1.9	< 2.4	-	178.7
V608	1.31	20.72	< 1.3	< 2.0	1.15	21.87	2.22 ± 0.17	< 1.6	g^+	71.0
V611	0.85	21.69	1.89 ± 0.19	< 1.4	1.35	25.14	< 2.0	4.13 ± 0.18	t	162.2
V626	0.79	20.75	2.05 ± 0.18	< 1.3	0.87	21.58	< 1.1	3.51 ± 0.20	t	169.7
V656	0.74	22.37	~ 1.9[d]	< 1.5[d]	1.10	24.18	< 2.0	3.77 ± 0.19	t	175.7
V666	0.88	19.66	~ 2.1[d]	< 1.5[d]	1.11	21.94	< 0.6	3.67 ± 0.21	t	170.1
V667	1.04	22.53	1.94 ± 0.16[e]	< 1.3	1.11	23.35	< 1.3	3.50 ± 0.20	t	174.6
V701[f]	1.03	21.39	0.73 ± 0.35	2.82 ± 0.24	1.02	19.73	1.05 ± 0.31	< 1.2	g^-	-65.8

[a] Chemical shifts (ppm) of ^1H and ^{13}C are referenced against external TSP. $^3J_{C\gamma N}$, $^3J_{C\gamma C'}$ values are in Hz; in cases where J values could not be measured due to the absence of cross-peaks in difference spectra, the upper bounds of $^3J_{C\gamma N}$ and $^3J_{C\gamma C'}$ were estimated based on the intensities of reference cross-peaks and assuming that the detection limit corresponds to 3.8 rmsd of baseline noise in difference spectra. The valine residues whose methyls could not be stereospecifically assigned using the method of fractional ^{13}C-labeling[11,12] and were assigned from the J coupling data are shown in red, while the valine residues that could not be stereospecifically assigned from J couplings due to rotamer averaging or noncanonical side chain conformations and were assigned using fractional ^{13}C-labeling are shown in blue. Residues in black could be assigned using either approach. Valine side chains where at least one of the diastereotopic methyl groups was found to undergo chemical exchange on the millisecond time scale[20] are shown in italics. Cross-peaks from methyls of V340, V389, and V620 had low signal-to-noise in all the reference data sets and were not observed in any of the difference spectra, while correlations involving V556 and V600 could not be quantified due to overlap of resonances; all these residues are, therefore, omitted from the table. [b] Dominant canonical rotameric states consistent with the measured J couplings: t - trans, g^+ - gauche$^+$, g^- - gauche$^-$; dash indicates that the preferred rotameric state could not be established from the measured J couplings. [c] The values of χ_1 angles are taken from the X-ray structure of glyoxylate-Mg^{2+}-bound MSG, PDB access code 1d8c,[45] unless indicated otherwise. [d] The value could not be measured (measured precisely) due to complete (partial) overlap. In cases where Val methyl resonances are overlapped in reference data sets, lower bounds for J values are reported. [e] The value could be measured only from the ZQ-SED data set. [f] Rotamer averaging or noncanonical χ_1 value is probable for this side chain ($^3J_{C\gamma C'}$ (trans) < 3.0 Hz and/or $^3J_{C\gamma N}$ (trans) < 1.5 Hz). [g] Rotamer averaging is apparent from the measured J values. [h] The value of χ_1 calculated from the X-ray coordinates of pyruvate-acetylCoA-bound MSG, PDB access code 1p7t.[46] [i] The coordinates of these side chains were not determined in any of the available X-ray structures of MSG.

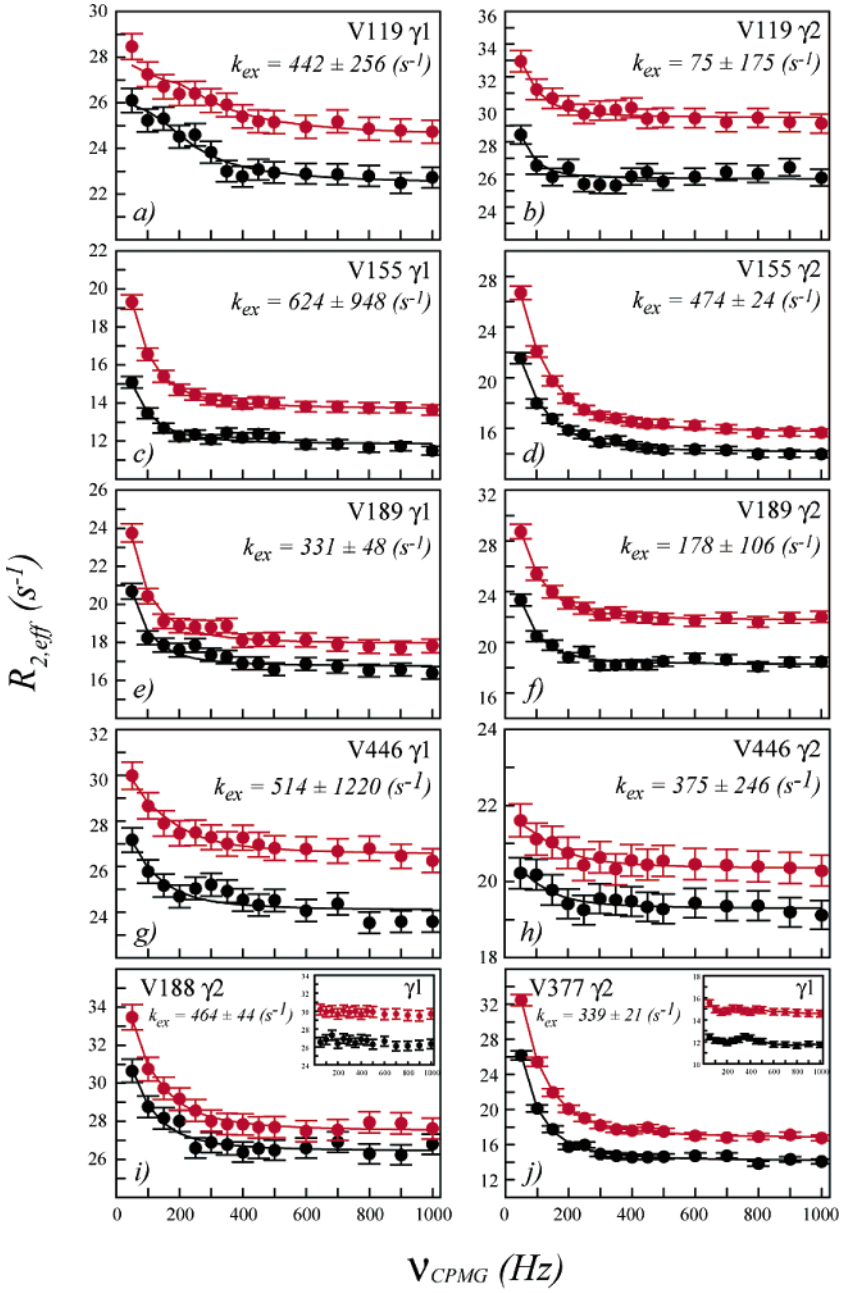

Figure 6. $^{1}H-^{13}C$ MQ relaxation dispersion profiles for selected Val residues that show evidence of rotamer averaging from measured values of $^{3}J_{C\gamma N}$ and $^{3}J_{C\gamma C'}$ couplings, Table 1. Dispersion profiles were recorded at 800 (red) and 600 (black) MHz as described in detail by Korzhnev et al..[20] Values of $R_{2,eff}$ were calculated for each CPMG frequency, $\nu_{cpmg} = 1/(4\delta)$, where 2δ is the spacing between successive 180° ^{13}C pulses applied during a constant-time interval of duration T; $R_{2,eff} = -1/T \ln\{I(\nu_{cpmg})/I(0)\}$, where $I(\nu_{cpmg})$ and $I(0)$ are the intensities of cross-peaks recorded with and without the interval T, respectively (see ref 20 for details). Dispersion profiles obtained at 600 and 800 MHz were fit together using an equation that takes into account changes in both ^{1}H and ^{13}C chemical shifts between exchanging states.[20] Values of k_{ex}, describing the assumed two-site exchange process, and associated errors are indicated in the upper right-hand corner of each plot.

of +70.9° from the X-ray coordinates. This valine is a part of the V118−V119−P120 sequence in the β1 strand of the β-barrel core domain of MSG and, together with the preceding V118, is within 8 Å of the glyoxylate binding site. Notably the ^{1}HN and ^{15}N chemical shifts of V119 undergo significant changes upon titration with pyruvate ($\Delta_{HN} = 0.53$ and $\Delta_{N} = 0.15$ ppm) or acetyl-CoA ($\Delta_{HN} = -0.30$ and $\Delta_{N} = -0.10$ ppm in a complex that is initially saturated with pyruvate).[8] It is perhaps not so surprising, therefore, that the ligated forms of the protein used for X-ray analyses[45,46] would show differences in this region with the apo-solution state considered here. Also of note, both methyls of V119 undergo conformational exchange on the millisecond time scale (see below) and also experience rotamer averaging, with the measured $^{3}J_{C\gamma 1C'}$ (2.56 ± 0.26 Hz, Table 1) value significantly lower than expected for a static, canonical gauche^{-} configuration.

Recently, Chou, Case, and Bax have published a comprehensive analysis of $^{3}J_{C\gamma N}$ and $^{3}J_{C\gamma C'}$ values from Val, Thr, and

(45) Howard, B. R.; Endrizzi, J. A.; Remington, S. J. *Biochemistry* **2000**, *39*, 3156−68.

(46) Anstrom, D. M.; Kallio, K.; Remington, S. J. *Protein Sci.* **2003**, *12*, 1822−1832.

Ile residues measured in a number of proteins and calculated populations of different rotameric states in ubiquitin.[19] The size of MSG, however, precludes such a detailed analysis of Val side chain conformations, especially since for many residues only approximate values of couplings could be obtained. We have, therefore, chosen to highlight Val side chains whose *J* values are apparently extensively averaged, possibly from fast "hopping" motions between the three staggered states (labeled with superscripts *g* in Table 1), and those whose set of *J* values indicates the presence of motional averaging, noncanonical side chain conformations (χ1 angles), and/or skewed populations of interconverting rotameric states (labeled with *f* in Table 1).

In an attempt to gain more insight into the nature of the dynamical processes that are suggested by the averaged coupling values (Table 1, residues labeled *f*,*g*), we have recorded $^{1}H-^{13}C$ MQ relaxation dispersion experiments that probe millisecond time scale dynamics at methyl positions in proteins.[20] Out of the 14 Val side chains in MSG that (very likely) experience rotamer averaging (*f*,*g* in Table 1), at least 1 methyl group in 10 of these residues (highlighted with italics in Table 1) undergoes slow conformational exchange on the millisecond time scale or is proximal to a residue that is dynamic in this time regime. Figure 6 shows relaxation dispersion profiles measured for methyls of V119, V155, V188, V189, V377, and V446 of MSG recorded at 600 and 800 MHz spectrometer frequencies. In many cases both methyl groups within the same Val residue give rise to similar dispersion profiles (Figure 6a−h). In a number of cases a flat profile is obtained for one of the methyls but not the second (Figure 6i and j). Such dispersions may be due to anisotropic methyl dynamics that modulate the chemical shifts of the two methyl carbons differently. Alternatively, in some cases the differences in the dispersions may reflect a situation where the conformational fluctuations of interest do not derive from motions involving the Val residue per se but from a group proximal to one of the two methyls that, therefore, modulates the chemical shifts of only that methyl. Interestingly, $^{3}J_{C\gamma N}$ and $^{3}J_{C\gamma C'}$ values measured for V166, V170, and V261 are consistent with a single rotameric state, although substantial dispersion profiles are measured for the $C_{\gamma 2}$ methyls of these residues (see Supporting Information). Modulations of chemical shifts from motions of neighboring sites would certainly be one possible explanation of such data. Finally, of note, the two Val residues whose side chains are missing from all of the X-ray structures of MSG[45,46] show extensive rotamer averaging (V155, V377) and have the highest R_{ex} values, 7.57(11.04) and 12.06(15.68) s^{-1} at 600(800) MHz, respectively.

The correlation between averaged scalar coupling values and millisecond time scale motions is striking especially considering that scalar couplings can be averaged by processes that span a wide range of time scales, with picosecond to millisecond time constants. A number of papers published recently using relatively small proteins have described approaches for quantifying the time scale of averaging. In one study, Millet et al. have examined side chain dynamics in a series of three mutants of protein L by a combination of ^{2}H spin relaxation methods and measurement of $^{3}J_{C\gamma N}$ and $^{3}J_{C\gamma C'}$ values.[36] In this study the full complement of five different ^{2}H relaxation rates[47,48] was recorded so that it was possible to separate contributions to relaxation from picosecond and nanosecond time scale dynamics. Those residues displaying nanosecond motions also showed extensive χ_1 averaging, while, with only one exception, those residues for which nanosecond motions were not detected in any of the three mutants had ^{3}J values consistent with a single canonical rotameric state.[36] These results are consistent with ^{3}J averaging processes on the nanosecond time scale. In a second study, Chou, Case, and Bax have shown a good correlation between generalized order parameters for the methyl $^{13}C-^{13}C$ bond vector calculated from a combination of scalar and dipolar couplings and order parameters from ^{2}H relaxation for ubiquitin.[19] For some residues, however, the estimate of order is larger from the ^{2}H data, suggesting that additional motions slower than the correlation time of the protein contribute to the ^{3}J averaging.[19] In the case of MSG, information about nanosecond time scale dynamics from ^{2}H-based experiments must await improvements in the methodology that substantially increase their sensitivity. Assuming, however, from the work on protein L described above that at least some of the averaging of ^{3}J values in MSG is on the nanosecond time scale, the present results suggest (not surprisingly) that residues showing side chain nanosecond dynamics often also have slower motions.

In summary, we have presented stereospecific assignments for approximately 90% of Leu and Val methyl groups in MSG. In the case of Leu methyls, assignments were obtained exclusively from the 10% ^{13}C-labeling methodology. A series of quantitative *J* based experiments, exploiting the sensitivity and resolution enhancements associated with methyl-TROSY spectroscopy, has been developed for measuring $^{3}J_{C\gamma N}$ and $^{3}J_{C\gamma C'}$ values of Val residues in high molecular weight proteins. Excellent agreement is obtained between rotameric states of apo-MSG in solution and the glyoxylate-bound protein.[45] In addition to stereospecific assignments and determination of rotameric states, ^{3}J values provide important information about Val side chain dynamics and, interestingly, a strong correlation between residues showing millisecond time scale motions from relaxation dispersion techniques and χ_1 averaging has been established.

Acknowledgment. This work was supported by a grant from the Canadian Institutes of Health Research (CIHR) to L.E.K. V.T. acknowledges the support of the Human Frontiers Science Program. L.E.K. holds a Canada Research Chair in Biochemistry.

Supporting Information Available: One table reporting stereospecific assignments of Leu methyl groups in MSG, one figure of an alternative pulse scheme for measurement of $^{3}J_{C\gamma C'}$, one figure illustrating the correlation of $^{3}J_{C\gamma C'}$ values obtained from different sequences, and one figure of $^{1}H-^{13}C$ MQ dispersions illustrating that residues with substantial dispersion profiles do not necessarily display rotamer averaging. This material is available free of charge via the Internet at http://pubs.acs.org.

JA048738U

(47) Millet, O.; Muhandiram, D. R.; Skrynnikov, N. R.; Kay, L. E. *J. Am. Chem. Soc.* **2002**, *124*, 6439−6448.
(48) Skrynnikov, N. R.; Millet, O.; Kay, L. E. *J. Am. Chem. Soc.* **2002**, *124*, 6449−6460.
(49) Levitt, M.; Freeman, R. *J. Magn. Reson.* **1978**, *33*, 473−476.
(50) Shaka, A. J.; Keeler, J.; Frenkiel, T.; Freeman, R. *J. Magn. Reson.* **1983**, *52*, 335−338.
(51) Kay, L. E.; Keifer, P.; Saarinen, T. *J. Am. Chem. Soc.* **1992**, *114*, 10663−10665.
(52) Geen, H.; Freeman, R. *J. Magn. Reson.* **1991**, *93*, 93−141.
(53) Patt, S. L. *J. Magn. Reson.* **1992**, *96*, 94−102.
(54) Boyd, J.; Soffe, N. *J. Magn. Reson.* **1989**, *85*, 406−413.
(55) Marion, D.; Ikura, M.; Tschudin, R.; Bax, A. *J. Magn. Reson.* **1989**, *85*, 393−399.